The targeted cytosolic degradation of class I histone deacetylases is essential for efficient alphaherpesvirus replication

Sheng-Li Ming[1,2,3#], Meng-Hua Du[1,2,3#], Jia-Ming Yang[6#], Ya-Di Guo[1,2,3], Jia-Jia Pan[1,2,3], Wei-Fei Lu[1,2,3], Jiang Wang[1,2,3,5], Lei Zeng[1,2,3*], Bei-Bei Chu[1,2,3,4,5*]

[1]College of Veterinary Medicine, Henan Agricultural University, Zhengzhou 450046, Henan Province, China

[2]Key Laboratory of Animal Biochemistry and Nutrition, Ministry of Agriculture and Rural Affairs, China

[3]Key Laboratory of Animal Growth and Development of Henan Province, Henan Agricultural University, Zhengzhou 450046, Henan Province, China

[4]International Joint Research Center of National Animal Immunology, Henan Agricultural University, Zhengzhou 450046, Henan Province, China

[5]Ministry of Education Key Laboratory for Animal Pathogens and Biosafety, Zhengzhou 450046, Henan Province, China

[6]State Key Laboratory of Membrane Biology, School of Pharmaceutical Sciences, Tsinghua University, Beijing 100084, China

[#]These authors contributed equally

[*]Correspondence: zenglei@henau.edu.cn (L. Zeng); chubeibei@henau.edu.cn (B.-B. Chu).

Abstract

Viral infection triggers a robust DNA damage response (DDR), reshaping the host chromatin landscape to facilitate viral replication. Here, we uncover a novel mechanism by which alphaherpesviruses exploit the DDR pathway. We demonstrated that herpes simplex virus 1 (HSV-1) and pseudorabies virus (PRV) induced selective degradation of class I histone deacetylases (HDAC1/2), leading to histone hyperacetylation and subsequent DDR activation. Strikingly, viral infection promoted nuclear export of HDAC1/2, followed by MDM2-mediated K63-linked polyubiquitination and proteasomal degradation in the cytoplasm. Pharmacological inhibition of either DDR signaling or HDAC1/2 nuclear export significantly affected viral replication *in vitro* and *in vivo*. Our findings reveal a unique viral strategy to hijack host epigenetic regulation for efficient replication and identify potential therapeutic targets for alphaherpesvirus infections.

Keywords: Alphaherpesviruses; HDACs; MDM2; Ubiquitination; DNA damage response.

Introduction

HSV-1 is a widespread neurotropic virus that infects more than two-thirds of the global population under the age of 50 [1, 2]. After initial infection of mucosal epithelia and neuronal tissues, HSV-1 establishes lifelong latency within sensory ganglia [1, 3]. Clinically, HSV-1 infection can present as oral or genital lesions and, in severe instances, may progress to herpes simplex encephalitis—a potentially fatal inflammation of the brain [4, 5]. Emerging evidence suggests a plausible association between HSV-1 and neurodegenerative conditions such as Alzheimer's disease, linking chronic neuroinflammation and neuronal impairment to persistent viral infection [6, 7]. To sustain lifelong infection, HSV-1 employs sophisticated strategies to evade host immune defenses and maintain latent reservoirs.

Epigenetic regulation plays a critical role in governing HSV-1 latency and reactivation [8, 9]. During latency, the virus coopts host histone deacetylases (HDACs) to enforce viral genomic silencing through chromatin condensation [10]. Although HDAC1 and HDAC2 are central to chromatin stability and DNA damage response (DDR), their roles during alphaherpesvirus infection appear complex and context-dependent. While these enzymes contribute to viral repression during latency [11], their potential involvement in promoting lytic replication—whether through degradation or functional inactivation—has remained inadequately explored.

Histone acetylation, a pivotal epigenetic modification that modulates chromatin accessibility and transcriptional activity, is dynamically regulated by histone acetyltransferases (HATs), which add acetyl groups to activate gene expression, and HDACs, which remove these groups to enforce repression [12, 13]. The HDAC family is categorized into four classes: Class I (HDAC1, 2, 3, 8), Class IIa/b, Class III (sirtuins), and Class IV (HDAC11) [14]. Among these, Class I HDACs—particularly HDAC1 and HDAC2—are indispensable for chromatin remodeling, genomic integrity, and immune modulation [15-17]. These enzymes contribute to host antiviral defense by fine-tuning the expression of immune-related genes. Nevertheless, the mechanisms through which HSV-1 overcomes this transcriptional repression remain incompletely

understood.

HDAC1 serves as a key regulator of chromatin dynamics and innate immune signaling, interfacing with critical pathways such as NF-κB, JAK-STAT, and Toll-like receptor cascades to shape antiviral responses [18-20]. For example, in lung epithelial cells, HDAC1 facilitates STAT1 phosphorylation and enhances interferon-stimulated gene (ISG) activation, thereby restricting influenza A virus replication [21, 22]. This underscores the dual function of HDAC1 in both epigenetic control and immune regulation. However, the specific strategies used by HSV-1 to manipulate HDAC1/2—particularly through ubiquitin-mediated degradation—to circumvent host immunity and enhance viral replication have not been clearly defined.

This study reveals that HSV-1 induces the degradation of HDAC1/2 via an MDM2-dependent ubiquitination mechanism, resulting in elevated histone acetylation, chromatin relaxation, and activation of DNA damage response pathways that collectively enhance viral replication. These findings offer novel insights into the epigenetic subversion strategies employed by HSV-1 and underscore the therapeutic potential of targeting the HDAC–MDM2 axis in the treatment of herpesvirus infections.

Materials and Methods

Mice

Female C57BL/6J mice (6–8 weeks old) were purchased from the Experimental Animal Center of Zhengzhou University (Zhengzhou, China) and housed in specific-pathogen-free facilities under controlled environmental conditions, including a 12-hour light-dark cycle and a temperature of 22°C. Following 15 days of infection, euthanasia was performed on the animals by administering pentobarbital sodium intravenously (90 mg/kg) in compliance with the recommendations of the Chinese Association for Laboratory Animal Sciences. The liver was excised for immunoblotting analysis, and the remaining bodies were disposed of harmlessly. All

procedures were in accordance.

Reagents and plasmids

Reagents were sourced as follows: Leptomycin B (HY-16909), MG-132 (HY-13259), 3-MA (HY-19312), cycloheximide (HY-12320), and chloroquine (HY-17589A) were purchased from MedChemExpress; berzosertib (S7102) was purchased from Selleck; DMSO (W387520) was purchased from Sigma-Aldrich. Antibodies against CHK1 (25887-1-AP), CHK2 (13954-1-AP), RAD51 (14961-1-AP), β-actin (66009-1-lg), P53 (10442-1-AP), HDAC1 (10197-1-AP), HDAC2 (12922-3-AP), HDAC4 (17449-1-AP), HDAC6 (12834-1-AP), HDAC11 (67949-1-Ig), and EGFP (50430-2-AP) were purchased from Proteintech; antibodies against p-P53 (9286), p-ATM (13050), ATM (2873), ATR (13934), p-ATR (2853), p-CHK1 (12302), p-CHK2 (2197), γ-H2AX (80312), H3 (4499), H4K8ac (2594), H4K12ac (13944), H4 (13919), H2AX (7631), H3K9ac (4658), H3K27ac (8173), UB (20326), and MDM2 (86934) were purchased from Cell Signaling Technology; H3K56ac antibody (07-677) was purchased from Millipore; ICP4 antibody (ab6514) was purchased from Abcam; ICP0 antibody (sc-53070) was purchased from Santa Cruz Biotechnology; FLAG antibody (F7425) was purchased from Sigma-Aldrich; HA antibody (A00169) was purchased from GenScript.

HDAC1 and HDAC2 coding sequences were amplified from HEK293 cell cDNA and cloned into p3×FLAG-CMV-10 to generate FLAG-tagged expression constructs. MDM2 coding sequence was amplified and inserted into pEGFP-C1 to produce EGFP-MDM2. Site-directed mutagenesis was performed using the QuikChange Site-Directed Mutagenesis Kit (Agilent Technologies, 200523) per the manufacturer's instructions to generate: FLAG-HDAC1 K8R, FLAG-HDAC1 K10R, FLAG-HDAC1 K31R, FLAG-HDAC1 K50R, FLAG-HDAC1 K58R, FLAG-HDAC1 K66R, FLAG-HDAC1 K74R, FLAG-HDAC1 K89R, FLAG-HDAC2 K75R, FLAG-HDAC1 (aa 1–329), FLAG-HDAC1 (aa 329–482), FLAG-HDAC1 (aa 1–100), FLAG-HDAC1 (aa 100–329), and EGFP-MDM2ΔRING (aa 1–435). HA-tagged ubiquitin constructs [HA-UB (WT), HA-UB (K48), HA-UB (K63)] were provided by

Dr. Bo Zhong (College of Life Sciences, Wuhan University, China).

Cells

Cell lines (HeLa/ATCC CL-82, Vero/ATCC CL-81, 3D4/21/ATCC CRL-2843, HEK293T/ATCC CRL-11268) were cultured in DMEM or RPMI 1640 supplemented with 10% fetal bovine serum (FBS), 1% penicillin/streptomycin, and 1% L-glutamine at 37°C under 5% CO_2 in a humidified incubator. For transient transfections, DNA constructs were delivered to HeLa and HEK293T cells using Lipofectamine 3000 (Invitrogen, L3000001) per the manufacturer's protocol.

To generate shRNA-mediated knockdown cell lines, HEK293T cells were co-transfected with control or gene-specific shRNA (Table S1), packaging plasmid psPAX2, and envelope plasmid pMD2.G. Post-transfection (6 h), medium was replaced, and lentiviral particles were harvested at 48 hours. Parental cells were infected with viral supernatant and selected with puromycin to establish stable knockdown lines

Viruses

HSV-1 strain F (provided by Dr. Chun-Fu Zheng, University of Calgary, Canada) and PRV-QXX were propagated per established protocols [23]. Viral titers were determined by plaque assays in Vero cells. For in vitro infections, cells were infected with HSV-1 or PRV-QXX at an MOI of 1. For in vivo studies, mice were intranasally inoculated with HSV-1 (1×10^6 pfu/mouse).

Immunoblotting, ubiquitination and Co-immunoprecipitation (Co-IP)

For immunoblotting, cells were lysed in RIPA buffer [50 mM Tris-HCl (pH 8.0), 150 mM NaCl, 1% Triton X-100, 1% sodium deoxycholate, 0.1% SDS, 2 mM $MgCl_2$] supplemented with protease/phosphatase inhibitors. Proteins were resolved by SDS-PAGE, transferred to PVDF membranes, and blocked with 5% nonfat milk in TBST (1 hour, RT). Membranes were incubated with primary antibodies (overnight, 4°C), then HRP-conjugated secondary antibodies (1 hour, RT). Signals were detected using Laminate Crescendo Western HRP Substrate (Millipore, Cat. No. WBLUR0500)

on a GE AI600 imager.

For ubiquitination assay, cells were lysed in IP buffer [50 mM Tris-HCl (pH 7.4), 150 mM NaCl, 1% NP-40, 1% sodium deoxycholate, 5 mM EDTA, 5 mM EGTA] and clarified (16,000 × *g*, 10 minutes, 4°C). Subsequently, 900 μl aliquots were incubated with 40 μl of a 1:1 slurry of Sepharose beads conjugated to anti-HDAC1 or anti-FLAG mouse monoclonal antibodies (4°C, 4 hours). Beads were washed four times with IP buffer, eluted in SDS sample buffer (10 minutes, boiling), and analyzed by immunoblotting.

For Co-IP assay, cells were lysed in Co-IP buffer [50 mM Tris-HCl (pH 7.4), 150 mM NaCl, 1% NP-40, 5 mM EDTA, 5 mM EGTA] and clarified (16,000 × *g*, 10 minutes, 4°C). Aliquots (900 μl) were incubated with 40 μl of a 1:1 slurry of Sepharose beads conjugated to IgG (GE Healthcare) or anti-FLAG mouse monoclonal antibody (4°C, 4 hours). Beads were washed three times with Co-IP buffer, eluted in SDS sample buffer (10 minutes, boiling), and analyzed by immunoblotting.

Immunofluorescence assay

Cells were fixed in 4% paraformaldehyde at room temperature for 20 min on coverslips in 12-well plates. Following three washes with PBS, cells were permeabilized with 0.2% Triton X-100 for 20 min and subsequently blocked with 10% FBS. Specific primary antibodies, diluted in 10% FBS, were then applied to the cells and incubated for 1 h at room temperature. After three PBS washes, cells were exposed to the appropriate secondary antibodies, also diluted in 10% FBS, for 1 h at room temperature. Nuclei were stained with DAPI for 5 min at room temperature, mounted using Prolong Diamond (Invitrogen), and visualized using a Zeiss LSM 800 confocal microscope.

Comet assay

Cells were seeded in 6-well plates and treated accordingly. Frosted microscope slides were coated with 0.5% normal melting point agarose. A mixture of 10 μL DMEM containing around 10,000 cells and 75 μL of 0.7% low melting point agarose was

layered onto the pre-coated agarose. An additional 75 μL of 0.7% low melting point agarose formed a third layer. The slides were lysed in a buffer containing 10 mM Tris-HCl, pH 10.0, 2.5 M NaCl, 100 mM Na2EDTA, 1% Triton X-100, and 10% DMSO for 2 hours at 4°C. Post-lysis, the slides were treated with an electrophoresis solution (300 mM NaOH, 1 mM Na2EDTA, pH >13) for 40 minutes, electrophoresed at 20 V (~300 mA) for 25 minutes, and neutralized with 0.4 mM Tris-HCl (pH 7.5). Subsequently, cells were stained with propidium iodide (PI, 5 μg/mL) and examined using a Zeiss LSM 800 confocal microscope. DNA damage was assessed based on tail moment using CometScore software.

qRT-PCR analysis

Total RNA was isolated using TRIzol reagent (TaKaRa) and reverse-transcribed into cDNA with the PrimeScript RT reagent kit (TaKaRa). qRT-PCR was performed in triplicate using SYBR Premix Ex Taq (TaKaRa) according to the manufacturer's protocol. Expression levels were normalized to β-actin as an internal reference. Melting curve analysis confirmed amplification specificity by verifying single-product formation in all reactions. Relative gene expression was calculated using the $2^{-\Delta\Delta Ct}$ method. Primer sequences are provided in Table S1

Plaque assay

Vero cells (seeded in six-well plates) were grown to confluence, infected with serially diluted viruses (10^{-1}–10^{-7}; 1 hour, 37°C), and washed with PBS to remove residual inoculum. DMEM containing 1% methylcellulose (4 mL/well) was added, and cells were incubated for 4–5 days. Post-incubation, cells were fixed with 4% paraformaldehyde (15 minutes), stained with 1% crystal violet (30 minutes), and plaques were quantified.

Statistical analysis

Statistical analyses were performed using GraphPad Prism 8 software. Comparisons between two groups were evaluated using a two-tailed Student's *t*-test. Significance was defined as $P < 0.05$. Data are presented as mean ± SD of three independent

experiments. Kaplan-Meier survival curves were generated and analyzed for mouse survival assessment.

Results

HSV-1 infection promotes HDAC1/2 degradation and histone hyperacetylation.

Post-translational modifications of histones play a critical role in regulating chromatin remodeling and gene expression. HDACs, a highly conserved enzyme family [21], catalyze the removal of acetyl groups from histones, thereby promoting chromatin condensation and transcriptional repression. To investigate the effect of HSV-1 infection on HDAC expression and histone acetylation, we examined the protein levels of key HDAC isoforms following viral infection. Immunoblotting analysis revealed a marked decrease in HDAC1 and HDAC2 protein levels in cells infected with either HSV-1 or PRV, whereas the expression of HDAC4, HDAC6, and HDAC11 remained unchanged (Fig. 1A, B). In contrast, qRT-PCR results showed no alterations in HDAC1 and HDAC2 mRNA levels (Fig. 1C, D), suggesting that their depletion is regulated at the post-translational level.

To assess the functional impact of HDAC1/2 reduction, we examined global histone acetylation patterns. Site-specific immunoblotting demonstrated elevated acetylation at multiple lysine residues, including H3K9, H3K27, H3K56, H4K8, and H4K12, in HSV-1-infected HeLa cells (Fig. 1E). A similar hyperacetylation profile was observed in PRV-infected 3D4/21 cells and in murine liver tissues infected with HSV-1 (Fig. 1F, G). Together, these findings indicate that HSV-1 selectively degrades class I HDACs, resulting in widespread histone hyperacetylation that fosters a chromatin state conducive to viral replication.

HSV-1 infection induces DDR through HDAC1/2 depletion and histone hyperacetylation.

Given that excessive histone acetylation can destabilize chromatin structure, we sought to elucidate the mechanism by which this epigenetic modification activates the DDR pathway. Accumulating evidence underscores the pivotal role of histone

modifications in maintaining genomic stability, with dynamic changes in chromatin architecture being intimately associated with DDR initiation. To determine whether HSV-1 infection induces DDR activation, we evaluated the phosphorylation of γ-H2AX, a well-established marker of DNA double-strand breaks. Immunofluorescence microscopy revealed a significant increase in γ-H2AX foci in cells infected with HSV-1 or PRV (Fig. 2A, B). Comet assays further corroborated enhanced DNA fragmentation under these conditions (Fig. 2C–F). Given the central role of ATM/ATR signaling in the DDR, we proceeded to examine the activation of key checkpoint kinases. Immunoblotting analysis confirmed phosphorylation of ATM, ATR, Chk1, Chk2, H2AX, and RAD51 in HSV-1-infected HeLa cells, 3D4/21 cells, and murine liver tissues (Fig. 2G, H).

Moreover, pharmacological inhibition of ATR using berzosertib markedly reduced viral titers in plaque assays (Fig. 2I). *In vivo*, administration of berzosertib significantly improved survival rates in HSV-1-infected mice (Fig. 2J). These results demonstrate that HSV-1 infection activates the DDR, likely mediated through HDAC1/2 degradation and consequent histone hyperacetylation. This virus-induced DDR activation underscores the profound impact of HSV-1 on host chromatin dynamics and genomic integrity.

HSV-1 promotes the ubiquitin-proteasome degradation of HDAC1/2.

To elucidate the mechanism responsible for HDAC1/2 degradation, we focused on their post-translational regulation. Since HDAC1/2 mRNA levels were unchanged after infection, we hypothesized that the reduction in HDAC1/2 protein is mediated through enhanced proteolytic degradation. To identify the relevant degradation pathway, HSV-1-infected HeLa cells were treated with either the proteasome inhibitor MG-132 or autophagy inhibitors (3-MA and chloroquine). Immunoblotting analysis indicated that only MG-132 rescued HDAC1/2 protein levels (Fig. 3A), confirming that degradation occurs primarily via the proteasomal pathway.

To examine whether HSV-1 infection induced ubiquitination of HDAC1, endogenous

immunoprecipitation assays were performed, which revealed increased ubiquitination of HDAC1 following infection (Fig. 3B). Subsequent ubiquitination assays using wild-type (WT), K48-only, and K63-only ubiquitin mutants demonstrated that HDAC1 undergoes K63-linked—but not K48-linked—polyubiquitination (Fig. 3C). Using a series of HDAC1 truncation mutants, we mapped the ubiquitination site to the N-terminal region (amino acids 1–100) (Fig. 3D–F). Site-directed mutagenesis further identified lysine 74 (K74) as the critical residue required for ubiquitination (Fig. 3G–I). Sequence alignment showed that HDAC2 K75 corresponds to HDAC1 K74 (Fig. 3J), and a K75R mutation in HDAC2 similarly abolished ubiquitination (Fig. 3J). Together, these results indicate that HSV-1 infection promotes K63-linked polyubiquitination of HDAC1/2 at conserved lysine residues, ultimately leading to their proteasomal degradation.

MDM2 functions as the E3 ligase mediating HDAC1/2 ubiquitination and degradation.

Having established the occurrence of K63-linked ubiquitination (Fig. 3), we next sought to identify the E3 ubiquitin ligase responsible. An RNAi screen targeting candidate E3 ligases revealed MDM2 as the principal mediator of HDAC1/2 degradation. Knockdown of MDM2—but not of PIRH2, KCTD11, CHFR, UHRF1, or TRIM46—effectively prevented HDAC1/2 depletion (Fig. 4A, B). Co-IP assay further confirmed an enhanced interaction between HDAC1 and MDM2 following HSV-1 infection (Fig. 4C).

To characterize this interaction, we focused on the RING finger domain of MDM2, which is essential for its E3 ligase activity. Co-IP analysis demonstrated that HSV-1 infection promoted binding between FLAG-HDAC1 and EGFP-MDM2, but not with a RING-deleted mutant (EGFP-MDM2ΔRING) (Fig. 4D), indicating that the interaction was RING domain-dependent. To identify the region within HDAC1 required for binding, HeLa cells were co-transfected with EGFP-MDM2 and either FLAG-HDAC1 or the ubiquitination-resistant mutant FLAG-HDAC1 K74R.

Infection with HSV-1 failed to induce binding between EGFP-MDM2 and the K74R mutant (Fig. 4E), underscoring the essential role of lysine 74 in mediating MDM2-dependent ubiquitination.

Ubiquitination assay further revealed that overexpression of EGFP-MDM2ΔRING did not enhance HSV-1-induced ubiquitination or degradation of HDAC1 (Fig. 4F). Similarly, the FLAG-HDAC1 K74R mutant remained resistant to ubiquitination under all experimental conditions (Fig. 4F). Collectively, these results demonstrate that HSV-1 induces HDAC1/2 degradation through MDM2-mediated K63-linked ubiquitination.

HSV-1 triggers cytoplasmic translocation of HDAC1 to facilitate its degradation.

To elucidate the mechanisms by which HSV-1 induces HDAC degradation, we systematically analyzed the subcellular localization of HDAC1. In mock-infected HeLa cells, HDAC1 was predominantly nuclear; however, HSV-1 infection triggered a pronounced translocation of HDAC1 to the cytoplasm (Fig. 5A). This redistribution was completely abolished by treatment with leptomycin B (LMB), a specific inhibitor of CRM1-mediated nuclear export (Fig. 5A).

To determine whether translocation is functionally linked to degradation, we conducted cycloheximide (CHX) chase assays. Degradation of both HDAC1 and HDAC2 began approximately 12 hours after CHX treatment and was markedly accelerated by HSV-1 infection (Fig. 5B). Importantly, LMB treatment restored degradation kinetics to levels comparable to those in mock-infected cells (Fig. 5B). Moreover, under LMB treatment, HSV-1 was unable to induce ubiquitination of endogenous HDAC1 (Fig. 5C).

Immunoblotting analysis further indicated that LMB suppressed HSV-1–induced phosphorylation of p53 and H2AX (Fig. 5E), confirming that CRM1-dependent nuclear export is essential for MDM2-mediated HDAC1 degradation. Notably, LMB treatment—which inhibits CRM1-dependent export and consequently prevents HDAC1 degradation—significantly impaired viral replication (Fig. 5F). Together,

these findings demonstrate that HSV-1 infection promotes cytoplasmic translocation of HDAC1, facilitating its ubiquitination and subsequent proteasomal degradation.

Discussion

HSV-1 manipulates host cellular pathways to facilitate its replication, latency, and reactivation [2]. In this study, we demonstrate that alphaherpesvirus targets class I histone deacetylases HDAC1 and HDAC2 for MDM2-mediated K63-linked polyubiquitination and subsequent proteasomal degradation. This degradation induces histone hyperacetylation, chromatin relaxation, and enhanced viral replication—revealing a mechanism through which alphaherpesvirus reprograms the host epigenetic landscape to optimize viral replication (Fig. 6).

Unlike human cytomegalovirus, which upregulates HDAC expression to suppress host immunity [24], HSV-1 promotes the degradation of HDAC1/2 to establish a chromatin environment conducive to viral transcription. This highlights a fundamental divergence in epigenetic strategies among herpesviruses. Our findings indicate that virus-directed degradation of HDAC1/2 occurs specifically during lytic replication [25], suggesting a dual role for these deacetylases: their presence supports latency, whereas their degradation facilitates lytic replication.

We identified MDM2 [26] as the principal E3 ubiquitin ligase responsible for ubiquitinating HDAC1 at lysine 74 and HDAC2 at lysine 75, leading to their proteasomal degradation. This mechanism is distinct from other E3 ligases, including PIRH2 [27] and TRIM46 [28]), and critically depends on the RING domain of MDM2. While K63-linked ubiquitination is typically associated with non-proteolytic functions, our work establishes its novel role in mediating HDAC1/2 degradation—uncovering a previously unrecognized viral pathogenesis pathway. Targeting this axis using MDM2 inhibitors or inhibiting nuclear export of HDAC1/2 significantly restricts viral replication, suggesting that host-directed antiviral strategies may help overcome resistance to direct-acting agents.

Depletion of HDAC1/2 increases acetylation at histone residues associated with open

chromatin and active transcription. Similar chromatin remodeling has been observed in other viral infections [29], underscoring its conserved role in viral gene regulation. Our results are consistent across multiple cell types, including HeLa, 3D4/21, and murine liver, emphasizing the central importance of HDAC1/2 suppression in HSV-1 biology. Notably, HDAC1/2 degradation activates DDR, as indicated by increased γ-H2AX foci and phosphorylation of ATM, ATR, Chk1, and Chk2. This aligns with previous reports that HSV-1 exploits DDR signaling to enhance replication [30-32]. Importantly, HDAC1/2 undergo CRM1-dependent nuclear export prior to degradation—a process inhibited by leptomycin B—highlighting the essential role of subcellular localization in viral manipulation of host proteins.

HSV-1–mediated HDAC1/2 degradation likely supports viral replication through multiple mechanisms, including evasion of nuclear antiviral sensors and stimulation of viral gene expression. Targeting the MDM2–HDAC1/2 axis represents a promising antiviral strategy. MDM2 inhibitors reduce HSV-1 titers [33] , suggesting that modulating ubiquitination pathways could complement existing therapies. Beyond herpesviruses, the MDM2–HDAC axis may be exploited by other DNA viruses (e.g., HBV, HPV) that manipulate chromatin and DDR, indicating a possible common host vulnerability. However, broad HDAC inhibition may unintentionally enhance viral replication, underscoring the need for targeted therapeutic approaches.

This study primarily employed in vitro models (e.g., HeLa and 3D4/21 cells), which lack the neuronal environment essential for studying HSV-1 latency. Future work should validate these findings in primary neurons and trigeminal ganglia [34]. Additional studies are also needed to determine whether HDAC1/2 degradation occurs during reactivation or is limited to lytic infection [8], and to explore the interplay between HDAC degradation, viral tegument proteins, and host stress responses. In vivo evaluation of inhibitors targeting the MDM2/HDAC1–2 pathway will be crucial for assessing their therapeutic potential.

Author contributions

Sheng-Li Ming and Meng-Hua Du : Data curation, Formal analysis, Investigation, Methodology, Validation, Visualization, Writing – original draft; Jia-Ming Yang: Data curation, Formal analysis, Investigation, Validation; Ya-Di Guo: Data curation, Formal analysis, Investigation, Validation, Visualization; Jia-Jia Pan: Data curation, Formal analysis, Investigation, Methodology, Visualization; Wei-Fei Lu: Data curation, Formal analysis, Investigation; Jiang Wang: Methodology, Visualization, Project administration, Supervision, Writing – review & editing; Lei Zeng and Bei-Bei Chu: Conceptualization, Data curation, Funding acquisi-tion, Investigation, Methodology, Project administration, Resources, Supervision, Validation, Writing – original draft, Writing – review & editing.

Declaration of competing interest

The authors declare that they have no competing interests.

Ethics statement

All procedures involving animals in this study received ethical approval from the Institutional Animal Care and Use Committee (IACUC) of Henan Agricultural University (Permit Number: HNND2020031008). This research was performed in accordance with the regulations specified in the Guide for the Care and Use of Laboratory Animals established by the Ministry of Science and Technology of China

Funding

This research was supported by grants from the National Key R&D Program of China (2021YFD1301200 and 2023YFD1801600), the China Postdoctoral Science Foundation (2025M770267, GZC20240430).

Data Availability Statement

The datas that support the findings of this study are openlyavailable in “Mendeley Data, V3” at https://data.mendeley.com/datasets/yg5fgtvxzk/3, doi: 10.17632/yg5fgtvxzk.3, reference number[35].

Declaration of generative AI and AI-assisted technologies in the writing process

This study affirms that neither generative artificial intelligence nor any other AI-assisted technologies were employed in the preparation of this manuscript.

References

1. Mohammed Tanveer H, Brent A S, David I B. Small Animal Models to Study Herpes Simplex Virus Infections. Viruses. 2024;16(7). doi: 10.3390/v16071037. PubMed PMID: 39066200.
2. Maria K. HSV-1 virions and related particles: biogenesis and implications in the infection. J Virol. 2025;99(3). doi: 10.1128/jvi.01076-24. PubMed PMID: 39898651.
3. Derek G, Daniel P D, Carol A H, Moriah L S, Paola K V, Mária B, et al. ICTV Virus Taxonomy Profile: Herpesviridae 2021. J Gen Virol. 2021;102(10). doi: 10.1099/jgv.0.001673. PubMed PMID: 34704922.
4. Jocelyne P, Guy B. Immunomodulatory Strategies in Herpes Simplex Virus Encephalitis. Clin Microbiol Rev. 2020;33(2). doi: 10.1128/cmr.00105-19. PubMed PMID: 32051176.
5. S M, Abhimanyu M, D D, P V, P M. Burden of herpes simplex virus encephalitis in the United States. J Neurol. 2017;264(6). doi: 10.1007/s00415-017-8516-x. PubMed PMID: 28516331.
6. Saba A, Francesca B. Targeting cyclooxygenases-1 and -2 in neuroinflammation: Therapeutic implications. Biochimie. 2010;93(1). doi: 10.1016/j.biochi.2010.09.009. PubMed PMID: 20868723.
7. Orhan A, Oliver U, Carmen I-D, Robert N, Frauke Z. Neuronal damage in brain inflammation. Arch Neurol. 2007;64(2). doi: 10.1001/archneur.64.2.185. PubMed PMID: 17296833.
8. David M K, Anna C. Chromatin control of herpes simplex virus lytic and latent infection. Nat Rev Microbiol. 2008;6(3). doi: 10.1038/nrmicro1794. PubMed PMID: 18264117.
9. Luis M S, MiYao H, Esteban Flores C, Kairui S. Chromatin-mediated epigenetic regulation of HSV-1 transcription as a potential target in antiviral therapy. Antiviral Res. 2021;192(0). doi: 10.1016/j.antiviral.2021.105103. PubMed PMID: 34082058.
10. Zhou G, Du T, Roizman B. HSV carrying WT REST establishes latency but reactivates only if the synthesis of REST is suppressed. Proceedings of the National Academy of Sciences of the United States of America. 2013;110(6):E498-506. doi: 10.1073/pnas.1222497110. PubMed PMID: 23341636.
11. Te D, Guoying Z, Shaniya K, Haidong G, Bernard R. Disruption of HDAC/CoREST/REST repressor by dnREST reduces genome silencing and increases virulence of herpes simplex virus. Proc Natl Acad Sci U S A. 2010;107(36). doi: 10.1073/pnas.1010741107. PubMed PMID: 20798038.
12. Patrick L, Joëlle T, Pascale T, Cécile C, Saadi K, Alberto L E. Functional interaction between class II histone deacetylases and ICP0 of herpes simplex virus type 1. J Virol. 2004;78(13). doi: 10.1128/jvi.78.13.6744-6757.2004. PubMed PMID: 15194749.
13. Brownell J, Zhou J, Ranalli T, Kobayashi R, Edmondson D, Roth S, et al. Tetrahymena histone acetyltransferase A: a homolog to yeast Gcn5p linking histone acetylation to gene activation. Cell. 1996;84(6):843-51. doi: 10.1016/s0092-8674(00)81063-6. PubMed PMID: 8601308.
14. Zijian L, Jingjing Y, Ruiyi M, Shijie X, Dan W, Rong Q, et al. Seneca Valley virus 3C protease cleaves HDAC4 to antagonize type I interferon signaling. J Virol. 2025;99(3). doi: 10.1128/jvi.02176-24. PubMed PMID: 39927774.
15. Hao-Ming C, Matthew P, Michelle H, Charles M R, Bryan R G W, Isabelle M, et al. Induction of interferon-stimulated gene expression and antiviral responses require protein deacetylase activity. Proc Natl Acad Sci U S A. 2004;101(26). doi: 10.1073/pnas.0400567101. PubMed PMID: 15210966.
16. Isabelle J M, Hao-Ming C, David E L. HDAC stimulates gene expression through BRD4 availability in response to IFN and in interferonopathies. J Exp Med. 2018;215(12). doi: 10.1084/jem.20180520.

460 PubMed PMID: 30463877.
461 17. Inna N, Curt M H. Interferon-stimulated transcription and innate antiviral immunity require
462 deacetylase activity and histone deacetylase 1. Proc Natl Acad Sci U S A. 2003;100(25). doi:
463 10.1073/pnas.2433987100. PubMed PMID: 14645718.
464 18. Ray S, Lee C, Hou T, Boldogh I, Brasier A. Requirement of histone deacetylase1 (HDAC1) in signal
465 transducer and activator of transcription 3 (STAT3) nucleocytoplasmic distribution. Nucleic acids
466 research. 2008;36(13):4510-20. doi: 10.1093/nar/gkn419. PubMed PMID: 18611949.
467 19. Li X, Li X, Huang P, Zhang F, Du J, Kong Y, et al. Acetylation of TIR domains in the TLR4-Mal-MyD88
468 complex regulates immune responses in sepsis. The EMBO journal. 2024;43(21):4954-83. doi:
469 10.1038/s44318-024-00237-8. PubMed PMID: 39294473.
470 20. Marques O, Horvat N, Zechner L, Colucci S, Sparla R, Zimmermann S, et al. Inflammation-driven
471 NF-κB signaling represses ferroportin transcription in macrophages via HDAC1 and HDAC3. Blood.
472 2025;145(8):866-80. doi: 10.1182/blood.2023023417. PubMed PMID: 39656097.
473 21. Leong J, Husain M. HDAC1 and HDAC2 Are Involved in Influenza A Virus-Induced Nuclear
474 Translocation of Ectopically Expressed STAT3-GFP. Viruses. 2024;17(1). doi: 10.3390/v17010033.
475 PubMed PMID: 39861822.
476 22. Kim Y, Ahn J. Positive role of promyelocytic leukemia protein in type I interferon response and its
477 regulation by human cytomegalovirus. PLoS pathogens. 2015;11(3):e1004785. doi:
478 10.1371/journal.ppat.1004785. PubMed PMID: 25812002.
479 23. Jiang W, Guo-Li L, Sheng-Li M, Chun-Feng W, Li-Juan S, Bing-Qian S, et al. BRD4 inhibition exerts
480 anti-viral activity through DNA damage-dependent innate immune responses. PLoS Pathog.
481 2020;16(3). doi: 10.1371/journal.ppat.1008429. PubMed PMID: 32208449.
482 24. Jane C M, Wolfgang F, Eric V, John H S. Control of cytomegalovirus lytic gene expression by
483 histone acetylation. EMBO J. 2002;21(5). doi: 10.1093/emboj/21.5.1112. PubMed PMID: 11867539.
484 25. Yuehong L, Shufeng L. A Cell Culture Model of Latent and Lytic Herpes Simplex Virus Type 1
485 Infection in Spiral Ganglion. ORL J Otorhinolaryngol Relat Spec. 2015;77(3). doi: 10.1159/000381679.
486 PubMed PMID: 26022499.
487 26. Kaifeng J, Yawei D, Jingtong X, Zhaopei L, Han Z, Xiaohe S, et al. Lethal clinical outcome and
488 chemotherapy and immunotherapy resistance in patients with urothelial carcinoma with MDM2
489 amplification or overexpression. J Immunother Cancer. 2025;13(1). doi: 10.1136/jitc-2024-010964.
490 PubMed PMID: 39762080.
491 27. Rocio Diaz E, Abhijeet A P, Jose F M-M, Akihiko U, Sean P M, Nayun K, et al. Pirh2-dependent DNA
492 damage in neurons induced by the G-quadruplex ligand pyridostatin. J Biol Chem. 2023;299(10). doi:
493 10.1016/j.jbc.2023.105157. PubMed PMID: 37579947.
494 28. Jicheng T, Xufeng P, Yong C, Yuzhou S, Chunyu J. TRIM46 activates AKT/HK2 signaling by modifying
495 PHLPP2 ubiquitylation to promote glycolysis and chemoresistance of lung cancer cells. Cell Death Dis.
496 2022;13(3). doi: 10.1038/s41419-022-04727-7. PubMed PMID: 35354796.
497 29. Julia M, Masih N, Thomas S, Sabrina S. Daxx and HIRA go viral - How chromatin remodeling
498 complexes affect DNA virus infection. Tumour Virus Res. 2025;(0). doi: 10.1016/j.tvr.2025.200317.
499 PubMed PMID: 40120981.
500 30. Max E M, David M K. Herpes Simplex Virus 1 Manipulates Host Cell Antiviral and Proviral DNA
501 Damage Responses. mBio. 2021;12(1). doi: 10.1128/mBio.03552-20. PubMed PMID: 33563816.
502 31. Daniel C A, Dipendra G, Kenric A G, William H C, Cary A M. Productive replication of human
503 papillomavirus 31 requires DNA repair factor Nbs1. J Virol. 2014;88(15). doi: 10.1128/jvi.00517-14.

504 PubMed PMID: 24850735.
505 32. Govind A S, Clodagh C OS. Viral and Cellular Genomes Activate Distinct DNA Damage Responses.
506 Cell. 2015;162(5). doi: 10.1016/j.cell.2015.07.058. PubMed PMID: 26317467.
507 33. Shengli M, Shijun Z, Jiayou X, Guoyu Y, Lei Z, Jiang W, et al. Alphaherpesvirus manipulates retinoic
508 acid metabolism for optimal replication. iScience. 2024;27(7). doi: 10.1016/j.isci.2024.110144.
509 PubMed PMID: 38989466.
510 34. Yue D, Yuqi L, Siyu C, Yuhang X, Hongjia C, Shuyuan Q, et al. Neuronal miR-9 promotes HSV-1
511 epigenetic silencing and latency by repressing Oct-1 and Onecut family genes. Nat Commun.
512 2024;15(1). doi: 10.1038/s41467-024-46057-6. PubMed PMID: 38443365.
513 35. Sheng-Li Ming M-HD, Jia-Ming Yang, Ya-Di Guo, Jia-Jia Pan, Wei-Fei Lu, Jiang Wang, Lei Zeng,
514 Bei-Bei Chu. The targeted cytosolic degradation of class I histone deacetylases is essential for efficient
515 alphaherpesvirus replication Mendeley Data. 2025. doi: 10.17632/yg5fgtvxzk.3.

516

517

Figure legends

Figure 1. Viral infection induces degradation of class I HDACs and hyperacetylation of histones H3 and H4.

(A) Immunoblotting analysis of the indicated HDACs in HeLa cells infected with HSV-1 (MOI = 1) for the indicated time points.

(B) Immunoblotting analysis of the indicated HDACs in 3D4/21 cells infected with PRV-QXX (MOI = 1) for the indicated time points.

(C and D) qRT-PCR analysis of *HDAC1* and *HDAC2* mRNA levels in HSV-1-infected HeLa cells (C) or PRV-QXX-infected 3D4/21 cells (D) (MOI = 1). Data are mean ± SEM; n = 3. $^{**}P < 0.01$, $^{***}P < 0.001$.

(E) Immunoblotting of the indicated proteins in HeLa cells from infected with HSV-1 (MOI = 1) for the indicated time points.

(F) Immunoblotting of the indicated proteins in 3D4/21 cells from infected with PRV-QXX (MOI = 1) for the indicated time points.

(G) Immunoblotting analysis of the indicated proteins in liver tissues from mice mock-infected or infected with HSV-1 (1×10^6 pfu per mouse) at 5 days post-infection (n = 3).

Figure 2. Viral infection triggers chromatin dysfunction and DDR activation via HDAC degradation.

(A and B) Immunofluorescence staining of γ-H2AX (red) and H2AX (green) in HSV-1-infected HeLa cells (A) or PRV-infected 3D4/21 cells (B) (MOI = 1). Scale bars: 10 μm.

(C and D) Comet assay assessing DNA damage in HeLa cells infected with HSV-1 (MOI = 1). Data are mean ± SEM; n = 40 cells/group. $^{**}P < 0.01$, $^{***}P < 0.001$.

(E and F) Comet assay assessing DNA damage in 3D4/21 cells infected with PRV (MOI = 1) at the indicated time points. Data are mean ± SEM; n = 40 cells/group. $^{**}P < 0.01$, $^{***}P < 0.001$.

(G and H) Immunoblotting analysis of DDR markers (p-ATM, p-ATR, p-Chk1,

p-Chk2, γ-H2AX) and viral ICP4/EP0 in HSV-1-infected HeLa cells (G) or PRV-QXX-infected 3D4/21 cells (H) (MOI = 1).

(I) Viral titers in HSV-1-infected HeLa cells (MOI = 1) treated with berzosertib (50 nM) or vehicle. Data are mean ± SEM; n = 3. *$P < 0.05$, **$P < 0.01$, ***$P < 0.001$

(J) Survival curves of HSV-1-infected mice (1×10^6 PFU/mouse) treated with berzosertib (20 mg/kg) or vehicle (n = 12/group), ***$P < 0.001$.

Figure 3. Viral infection induces K63-linked ubiquitination of HDAC1/2.

(A) Immunoblotting analysis of the indicated proteins in HeLa cells either mock-infected or infected with HSV-1 (MOI = 1), treated with vehicle, 3-MA (10 μM), MG-132 (10 μM), or chloroquine (10 μM) for the indicated times.

(B) Ubiquitination assay of HDAC1 in HeLa cells either mock-infected or infected with HSV-1 (MOI = 1) at 24 hpi.

(C) Ubiquitination assay of FLAG-HDAC1 in HeLa cells transfected with HA-ubiquitin variants (WT, K48, K63), and either mock-infected or infected with HSV-1 (MOI = 1) at 24 hpi.

(D) Schematic representation of HDAC1 deletion mutants.

(E-I) Ubiquitination assays of FLAG-HDAC1 mutant variants in HeLa cells either mock-infected or infected with HSV-1 (MOI = 1) at 24 hpi.

(J) Ubiquitination assays of FLAG-HDAC2 variants (WT and K75R) in HeLa cells either mock-infected or infected with HSV-1 (MOI = 1) at 24 hpi.

Figure 4. MDM2 mediates viral-induced HDAC1/2 degradation via K74/K75 ubiquitination.

(A) qRT-PCR analysis validation of E3 ligase knockdown efficiency (shPIRH2, shKCTD11, shMDM2, shCHFR, shUHRF1, shTRIM46) in HeLa cells. Data are mean ± SEM; n = 3. ***$P < 0.001$.

(B) Immunoblotting analysis of HDAC1/2 stability in E3 ligase-knockdown HeLa cells infected with HSV-1 (MOI = 1).

(C) Co-IP assay of endogenous HDAC1-MDM2 interaction in HSV-1-infected HeLa

cells (MOI = 1; 24 hpi).

(D) Co-IP assay of FLAG-HDAC1 with EGFP-MDM2 (WT or ΔRING) in HSV-1-infected HeLa cells (MOI = 1; 24 hpi).

(E) Co-IP assay of FLAG-HDAC1 (WT or K74R) with EGFP-MDM2 in HSV-1-infected HeLa cells (MOI = 1; 24 hpi).

(F) Ubiquitination assays of FLAG-HDAC1 (WT or K74R) co-expressed with EGFP-MDM2 (WT or ΔRING) in HSV-1-infected HeLa cells (MOI = 1; 24 hpi).

Figure 5. Cytoplasmic translocation enables MDM2-mediated HDAC1 degradation.

(A) Immunofluorescence staining of HDAC1 (red) and viral ICP4 (green) in HSV-1-infected HeLa cells (MOI = 1) ± leptomycin B (LMB; 10 nM; 24 h). Scale bar: 10 μm.

(B) CHX chase assay measuring HDAC1/2 degradation kinetics in HSV-1-infected HeLa cells (MOI = 1) ± LMB (10 μM).

(C) Ubiquitination assay of HDAC1 in HSV-1-infected HeLa cells (MOI = 1) ± LMB (10 μM; 24 h).

(D) Immunofluorescence analysis of MDM2 (red) and ICP4 (green) in HSV-1-infected HeLa cells (MOI = 1) ± LMB (10 μM; 24 h). Scale bar: 10 μm.

(E) Immunoblotting analysis of DDR markers (γ-H2AX) and HDAC1/2 in HSV-1-infected HeLa cells (MOI = 1) ± LMB (10 μM).

(F) Viral titers in HSV-1-infected HeLa cells (MOI = 1) ± LMB (10 μM). Data are mean ± SEM; n = 3. *$P < 0.05$, **$P < 0.01$, ***$P < 0.001$

Figure 6. A schematic model showing the targeted cytosolic degradation of class I histone deacetylases is essential for efficient alphaherpesvirus replication.

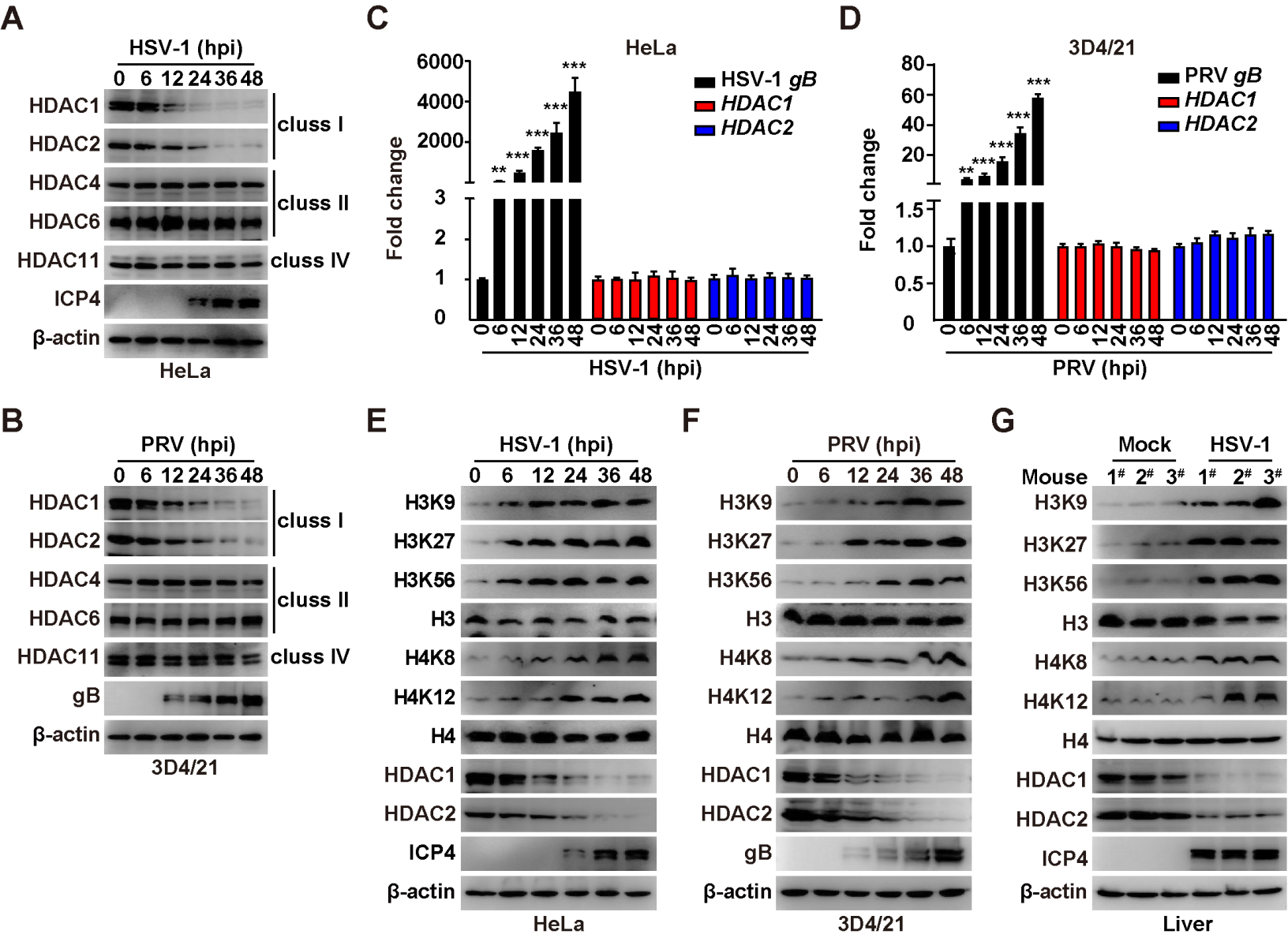
A
HSV-1 (hpi)
0 6 12 24 36 48
HDAC1
HDAC2
HDAC4
HDAC6
HDAC11
ICP4
β-actin
cluss I
cluss II
cluss IV
HeLa
B
PRV (hpi)
0 6 12 24 36 48
HDAC1
HDAC2
HDAC4
HDAC6
HDAC11
gB
β-actin
cluss I
cluss II
cluss IV
3D4/21
C
HeLa
Fold change
HSV-1 gB
HDAC1
HDAC2
HSV-1 (hpi)
D
3D4/21
Fold change
PRV gB
HDAC1
HDAC2
PRV (hpi)
E
HSV-1 (hpi)
0 6 12 24 36 48
H3K9
H3K27
H3K56
H3
H4K8
H4K12
H4
HDAC1
HDAC2
ICP4
β-actin
HeLa
F
PRV (hpi)
0 6 12 24 36 48
H3K9
H3K27
H3K56
H3
H4K8
H4K12
H4
HDAC1
HDAC2
gB
β-actin
3D4/21
G
Mock
HSV-1
Mouse
1# 2# 3# 1# 2# 3#
H3K9
H3K27
H3K56
H3
H4K8
H4K12
H4
HDAC1
HDAC2
ICP4
β-actin
Liver

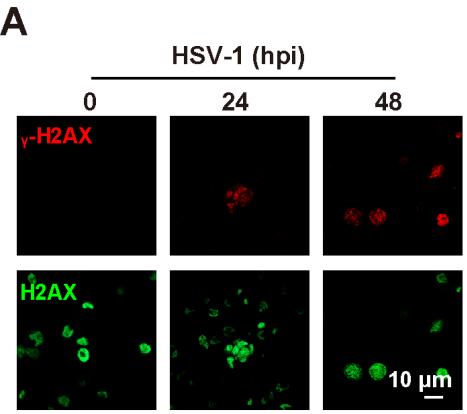
A
HSV-1 (hpi)
0
24
48
γ-H2AX
H2AX
10 μm

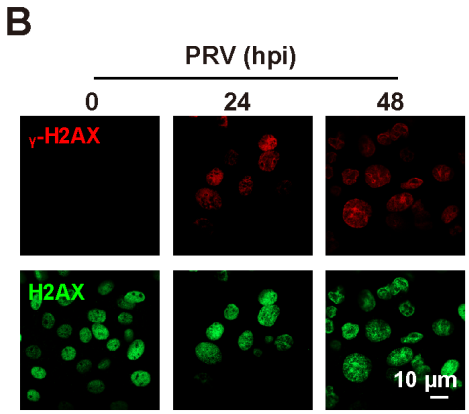
B
PRV (hpi)
0
24
48
γ-H2AX
H2AX
10 μm

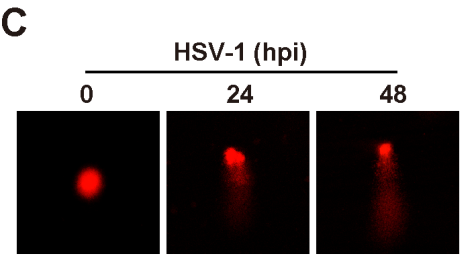
C
HSV-1 (hpi)
0
24
48

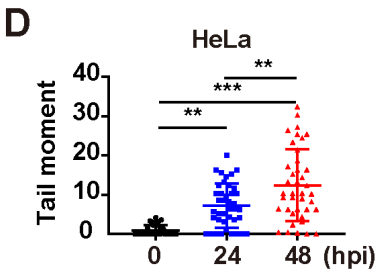
D
HeLa
Tail moment
40
30
20
10
0
**
***
**
0
24
48
(hpi)

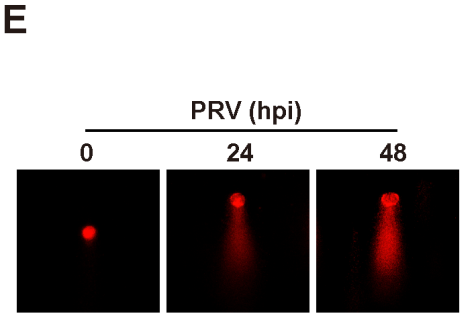
E
PRV (hpi)
0
24
48

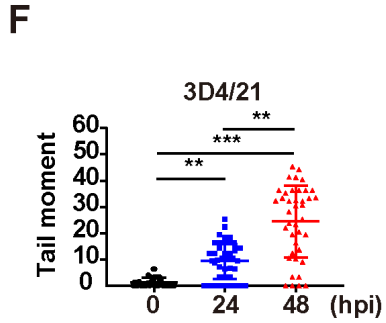
F
3D4/21
Tail moment
60
50
40
30
20
10
0
**
***
**
0
24
48
(hpi)

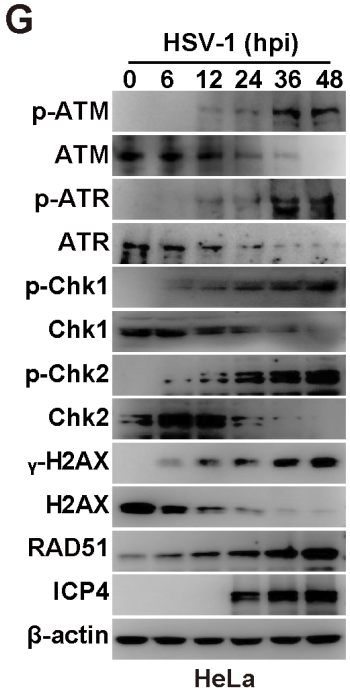
G
HSV-1 (hpi)
0 6 12 24 36 48
p-ATM
ATM
p-ATR
ATR
p-Chk1
Chk1
p-Chk2
Chk2
γ-H2AX
H2AX
RAD51
ICP4
β-actin
HeLa

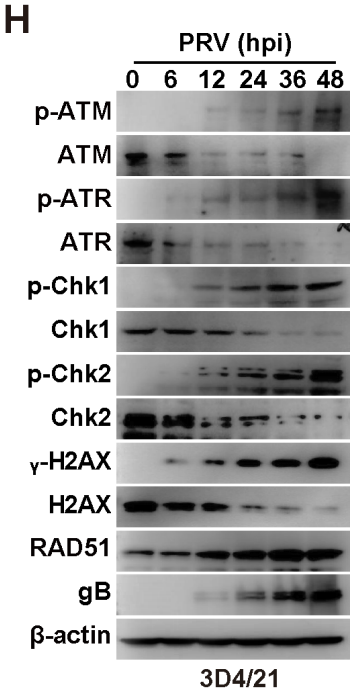
H
PRV (hpi)
0 6 12 24 36 48
p-ATM
ATM
p-ATR
ATR
p-Chk1
Chk1
p-Chk2
Chk2
γ-H2AX
H2AX
RAD51
gB
β-actin
3D4/21

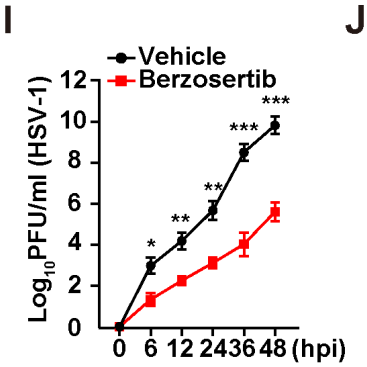
I
Vehicle
Berzosertib
Log10PFU/ml (HSV-1)
12
10
8
6
4
2
0
*
**
**
***
***
0 6 12 24 36 48 (hpi)

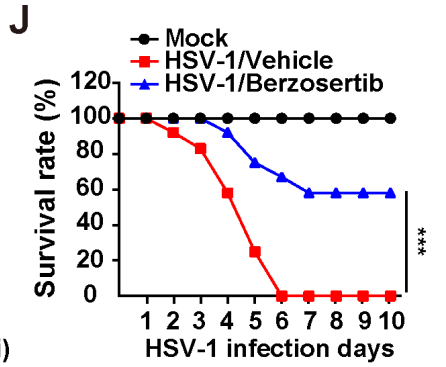
J
Mock
HSV-1/Vehicle
HSV-1/Berzosertib
Survival rate (%)
120
100
80
60
40
20
0
***
1 2 3 4 5 6 7 8 9 10
HSV-1 infection days

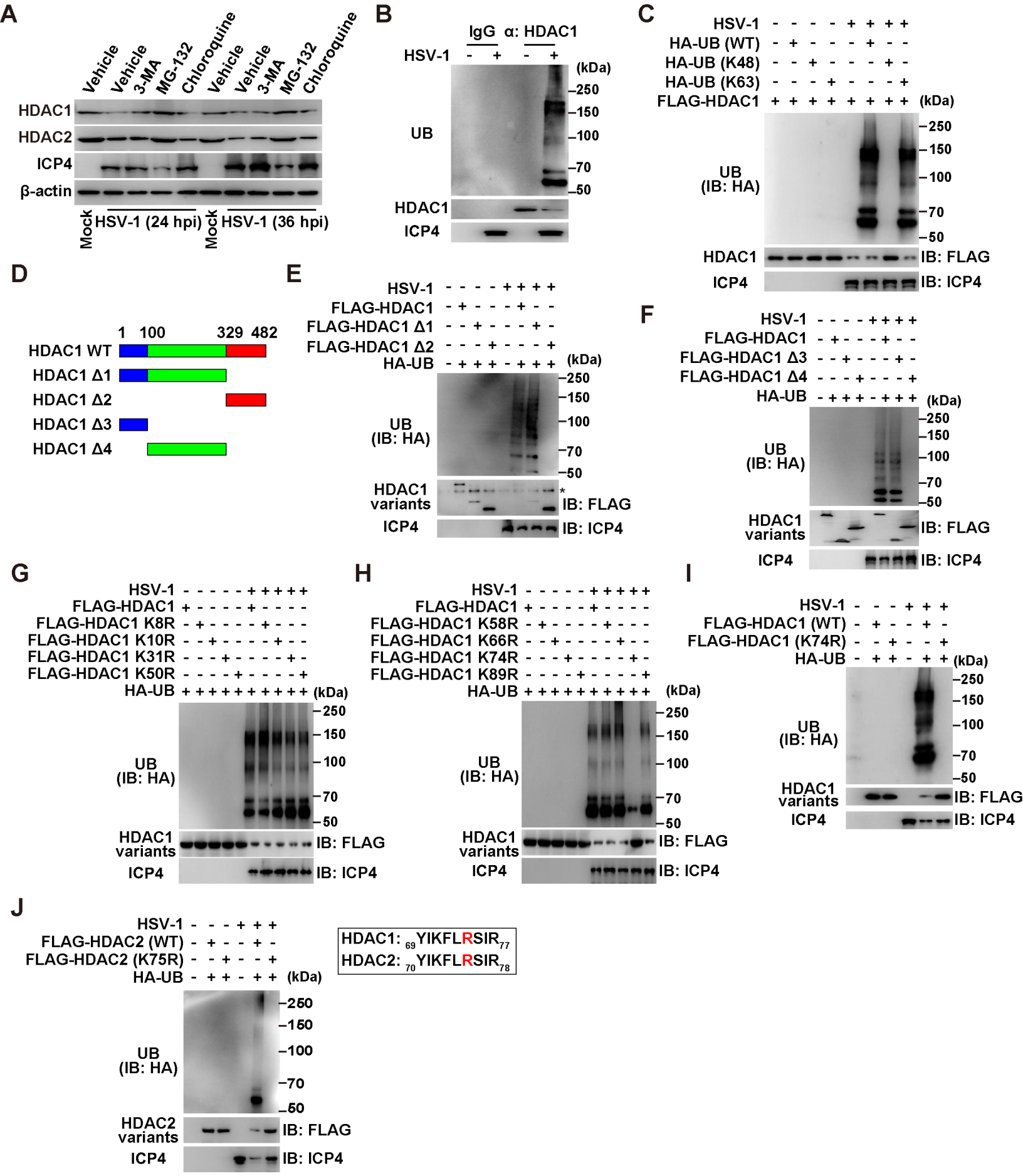
A
Vehicle
Vehicle
3-MA
MG-132
Chloroquine
Vehicle
Vehicle
3-MA
MG-132
Chloroquine
HDAC1
HDAC2
ICP4
β-actin
Mock
HSV-1 (24 hpi)
Mock
HSV-1 (36 hpi)
B
IgG
α: HDAC1
HSV-1
(kDa)
UB
HDAC1
ICP4
C
HSV-1
HA-UB (WT)
HA-UB (K48)
HA-UB (K63)
FLAG-HDAC1
(kDa)
UB
(IB: HA)
HDAC1
IB: FLAG
ICP4
IB: ICP4
D
1
100
329
482
HDAC1 WT
HDAC1 Δ1
HDAC1 Δ2
HDAC1 Δ3
HDAC1 Δ4
E
HSV-1
FLAG-HDAC1
FLAG-HDAC1 Δ1
FLAG-HDAC1 Δ2
HA-UB
(kDa)
UB
(IB: HA)
HDAC1
variants
IB: FLAG
ICP4
IB: ICP4
F
HSV-1
FLAG-HDAC1
FLAG-HDAC1 Δ3
FLAG-HDAC1 Δ4
HA-UB
(kDa)
UB
(IB: HA)
HDAC1
variants
IB: FLAG
ICP4
IB: ICP4
G
HSV-1
FLAG-HDAC1
FLAG-HDAC1 K8R
FLAG-HDAC1 K10R
FLAG-HDAC1 K31R
FLAG-HDAC1 K50R
HA-UB
(kDa)
UB
(IB: HA)
HDAC1
variants
IB: FLAG
ICP4
IB: ICP4
H
HSV-1
FLAG-HDAC1
FLAG-HDAC1 K58R
FLAG-HDAC1 K66R
FLAG-HDAC1 K74R
FLAG-HDAC1 K89R
HA-UB
(kDa)
UB
(IB: HA)
HDAC1
variants
IB: FLAG
ICP4
IB: ICP4
I
HSV-1
FLAG-HDAC1 (WT)
FLAG-HDAC1 (K74R)
HA-UB
(kDa)
UB
(IB: HA)
HDAC1
variants
IB: FLAG
ICP4
IB: ICP4
J
HSV-1
FLAG-HDAC2 (WT)
FLAG-HDAC2 (K75R)
HA-UB
(kDa)
UB
(IB: HA)
HDAC2
variants
IB: FLAG
ICP4
IB: ICP4
HDAC1: 69YIKFLRSIR77
HDAC2: 70YIKFLRSIR78

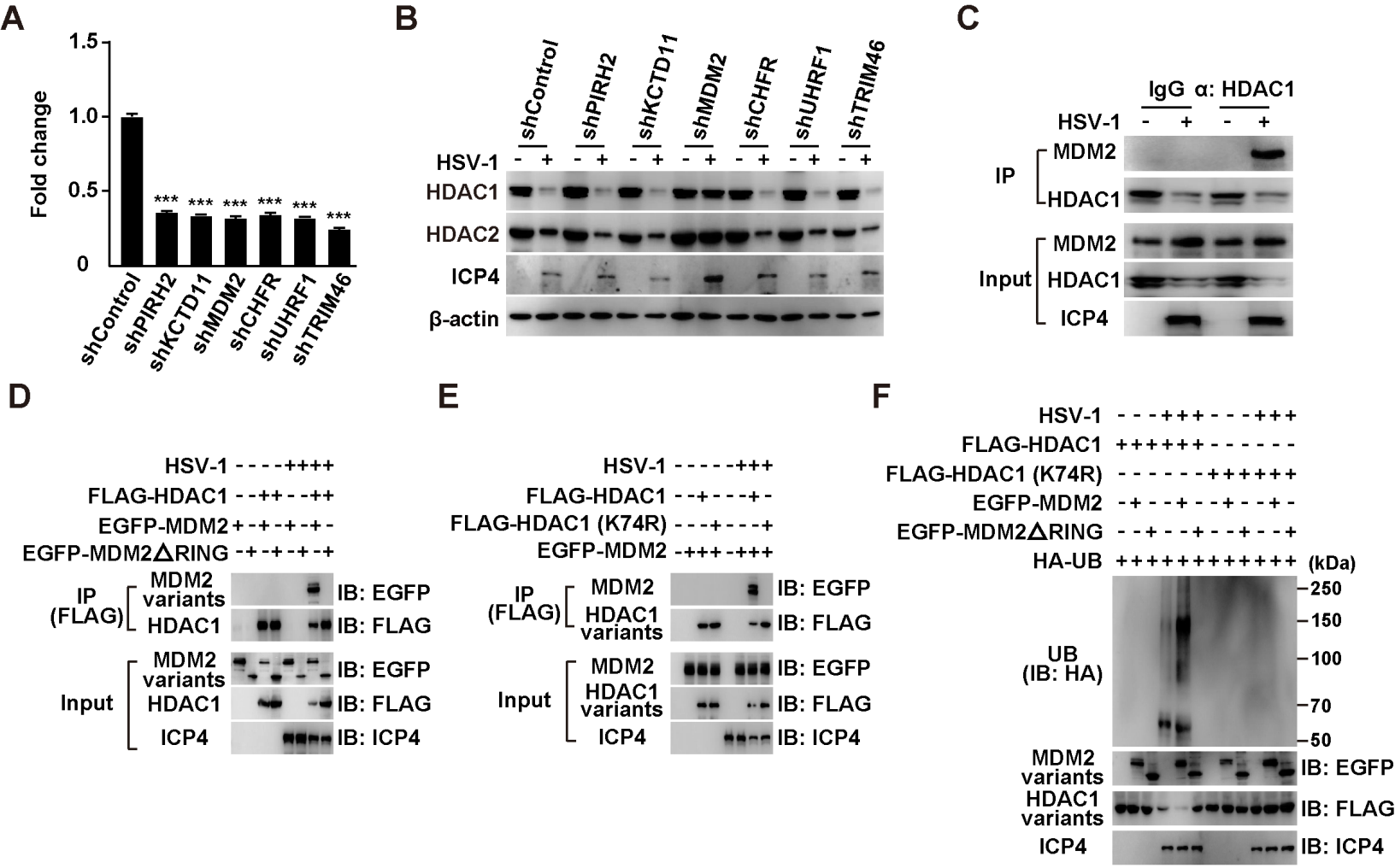
A
Fold change
1.5
1.0
0.5
0
***
shControl
shPIRH2
shKCTD11
shMDM2
shCHFR
shUHRF1
shTRIM46
B
HSV-1
HDAC1
HDAC2
ICP4
β-actin
C
IgG
α: HDAC1
IP
MDM2
HDAC1
Input
ICP4
D
HSV-1
FLAG-HDAC1
EGFP-MDM2
EGFP-MDM2△RING
IP (FLAG)
MDM2 variants
HDAC1
IB: EGFP
IB: FLAG
Input
ICP4
IB: ICP4
E
FLAG-HDAC1 (K74R)
HDAC1 variants
F
HA-UB
(kDa)
250
150
100
70
50
UB (IB: HA)

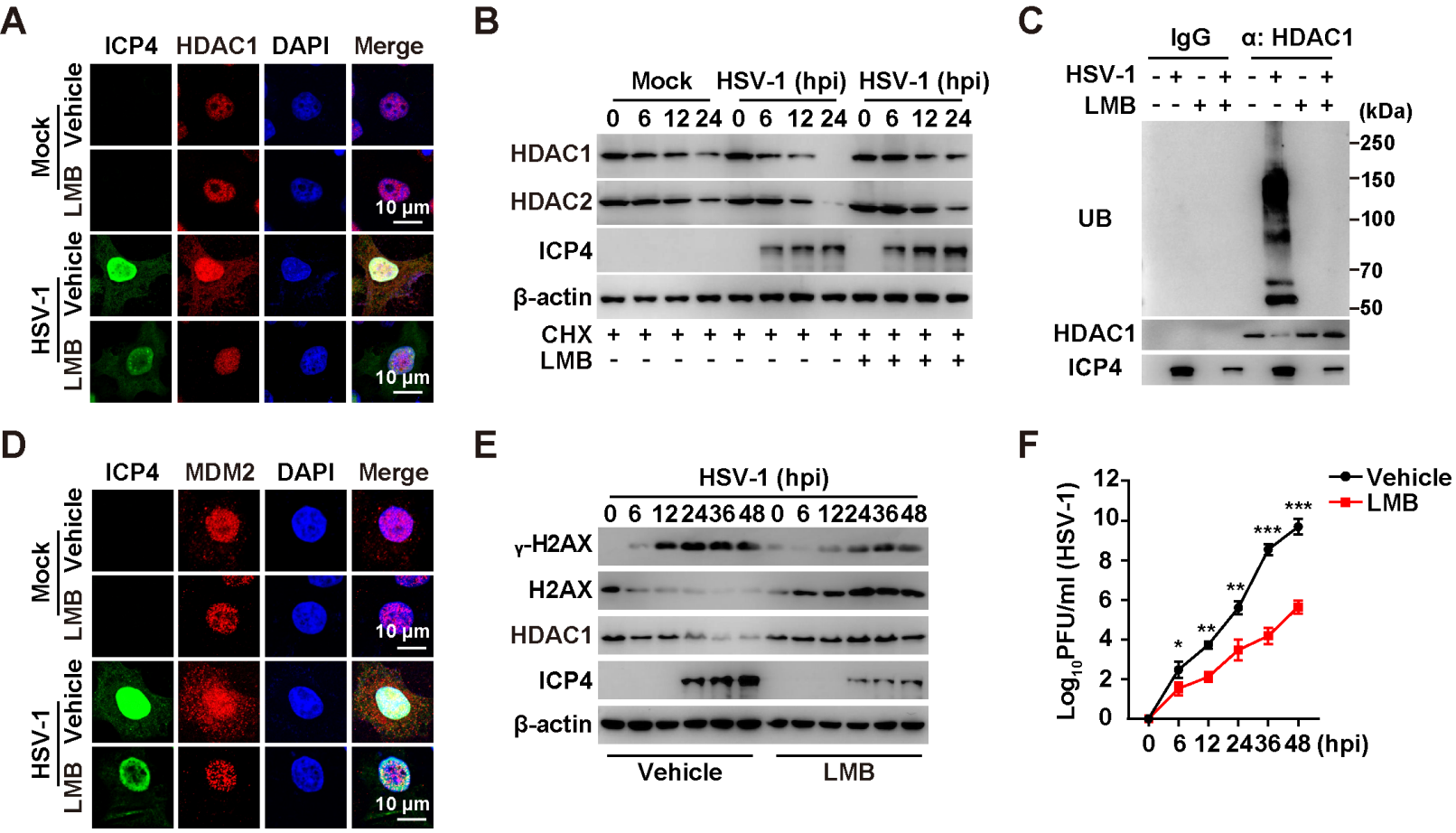
A
ICP4
HDAC1
DAPI
Merge
Mock
Vehicle
LMB
HSV-1
Vehicle
LMB
10 μm
10 μm
B
Mock
HSV-1 (hpi)
HSV-1 (hpi)
0 6 12 24 0 6 12 24 0 6 12 24
HDAC1
HDAC2
ICP4
β-actin
CHX + + + + + + + + + + + +
LMB - - - - - - - - + + + +
C
IgG
α: HDAC1
HSV-1 - + - + - + - +
LMB - - + + - - + +
(kDa)
250
150
100
70
50
UB
HDAC1
ICP4
D
ICP4
MDM2
DAPI
Merge
Mock
Vehicle
LMB
HSV-1
Vehicle
LMB
10 μm
10 μm
E
HSV-1 (hpi)
0 6 12 24 36 48 0 6 12 24 36 48
γ-H2AX
H2AX
HDAC1
ICP4
β-actin
Vehicle
LMB
F
Vehicle
LMB
Log10PFU/ml (HSV-1)
0 2 4 6 8 10 12
0 6 12 24 36 48 (hpi)
*
**
**
***
***

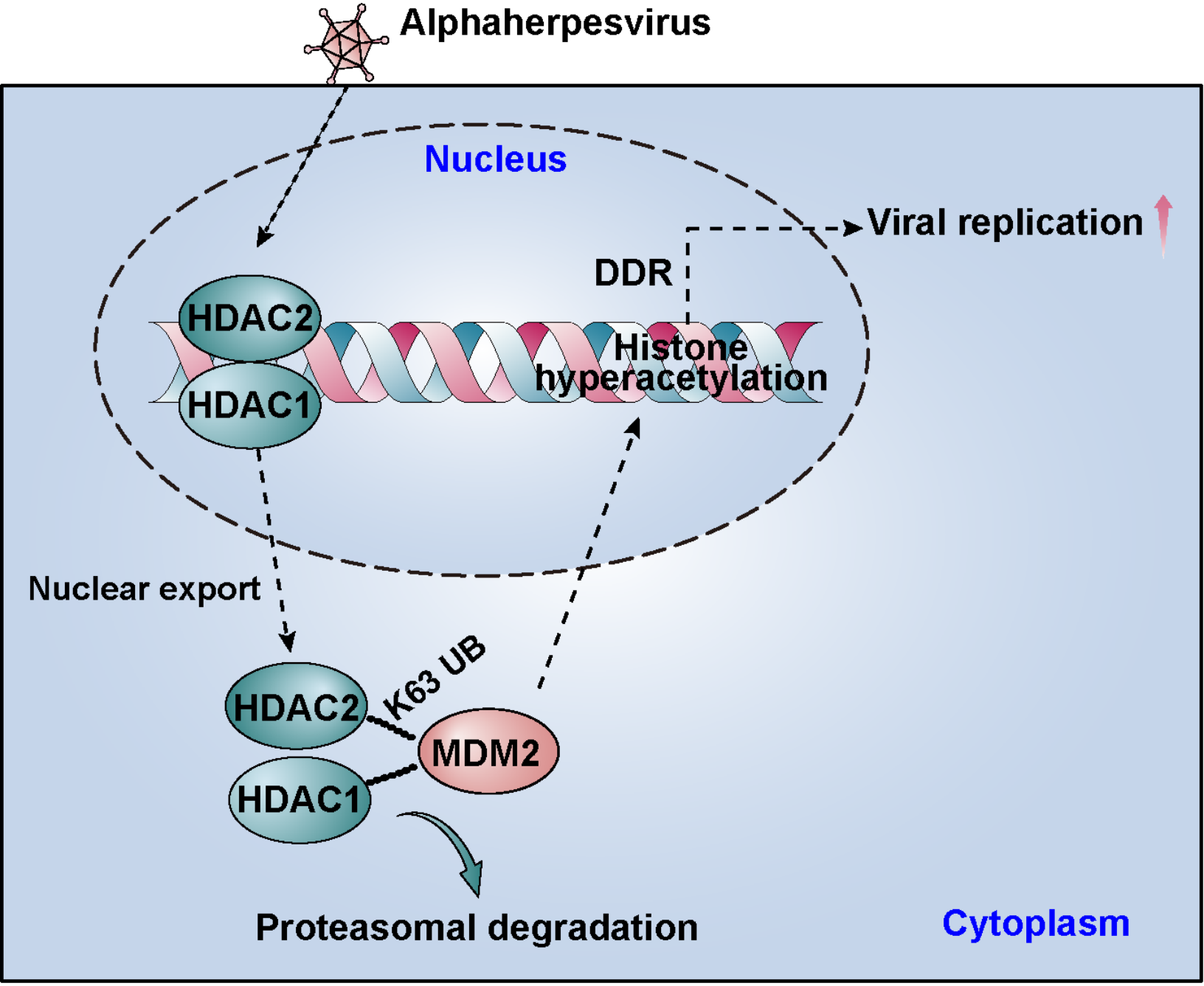
Alphaherpesvirus
Nucleus
Viral replication
DDR
HDAC2
HDAC1
Histone
hyperacetylation
Nuclear export
K63 UB
HDAC2
MDM2
HDAC1
Proteasomal degradation
Cytoplasm